

A Novel Coupling between the Electron Structure and Properties of Perovskite Transition Metal Oxides

Ghous Narejo, Warren F. Perger

Electrical Engineering Department, Michigan Tech University, Houghton, USA
Email: wfp@mtu.edu

Received August 2, 2012; revised January 5, 2013; accepted January 12, 2013

Copyright © 2013 Ghous Narejo, Warren F. Perger. This is an open access article distributed under the Creative Commons Attribution License, which permits unrestricted use, distribution, and reproduction in any medium, provided the original work is properly cited.

ABSTRACT

The *ab-initio* computational techniques are employed to extract the coupling between the electronic structure and magnetic properties for a wide variety of transition metal oxides. Optimized crystalline structures are computed by employing Hartree Fock (HF) and Density Functional Theory (DFT) techniques. The hydrostatic pressure is employed upon the optimized cubic crystalline structures of BaScO₃, BaTiO₃, BaVO₃, BaCrO₃, BaMnO₃ and BaFeO₃ to extract the coupling between the electronic structures and magnetic properties originating due to electron spin polarizations.

Keywords: Coupling; Spin; Strain

1. Introduction

The transition metals and their oxides are widely investigated by researchers [1-5]. The researchers employed the empirical, analytical and experimental methods [1-8] to extract the correlation between the electronic structures and properties of these materials. However, no major success has been reported in finding out the exact relationship between the crystalline structure and properties of these materials. We have attempted to investigate the complex nature of this interdependence existing in highly correlated physics of these materials. The complexity in these investigations arises due to an interaction between the electronic structures and properties. The latter are partially based upon the position of valence electrons in highly localized *d*-orbitals. This article explores the novel cubic perovskite phases for a wide variety of oxides of Sc-Fe. Later on, the interaction between these novel perovskite crystalline structures is compared with the computational results from other sources. An attempt has also been made to extract the interactions between the electronic structures and magnetic properties arising from electron spin polarization.

2. Computational Methods and Parameters

The Crystal09 code is employed to compute the exchange energy for the ferromagnetic and antiferromagnetic phases in each of the transition metal oxides. **Fig-**

ures 1 and 2 show the periodic crystalline lattice of perovskite cubic BaTiO₃ and BaFeO₃ consisting of the supercells of an optimum size utilized during these computations. These super cells were employed to compute the optimized crystalline structure and its interaction with electronic properties arising out of the electron spin polarization. Hydrostatic strains are employed for a varying sizes of electronic structures around optimized crystalline volume for each perovskite. During these computations the electronic basis sets for Ba and O were kept same. for BaScO₃, BaVO₃, BaCrO₃ and BaMnO₃ to facilitate the SCF convergence.

The computational results are reported in **Tables 1-5** and shown in **Figures 1-8**. The optimized crystalline structure is compared with experimental values if available and four additional computations of electronic structures and properties are performed. The hydrostatic compression or expansion of each crystalline structure is achieved by employing expansions and reductions of volume in small increments.

In this way, five separate computations are done for each of the crystalline systems. These computations are repeated for a large variety of crystalline systems to check the consistency.

Model

Some researchers [5,7,8] have proposed working theoretical models for a wide variety of transition metal oxides

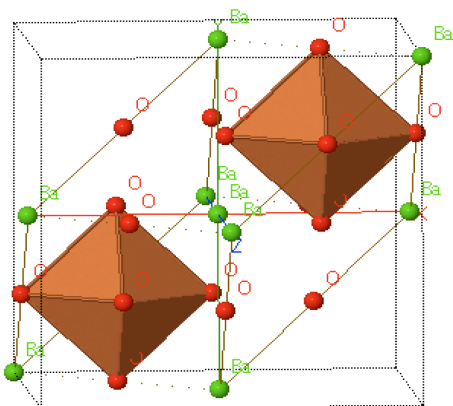


Figure 1. An octahedral is formed by O atoms having Fe atom in the middle. Green and red color spheres represent Ba, O and Fe atoms could not be seen as these are positioned in the middle of each cage in a perovskite BaFeO_3 .

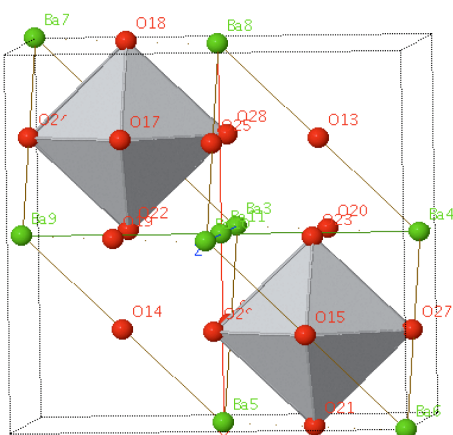


Figure 2. An octahedral is formed by O atoms having Fe atom in the middle. Green and red color spheres represent Ba and O while grey colored Ti atoms are positioned in the middle of each cage in a perovskite BaTiO_3 .

Table 1. Computations of E_{fm} , E_{exch}^{fm} , E_{afm} and E_{exch}^{afm} are done for lattice constant a in cubic BaScO_3 . The units of energy are in Hartree.

| $a(\text{\AA})$ | E_{exch}^{fm} | E_{exch}^{afm} | δ |
|-----------------|-----------------|------------------|----------|
| 4.120 | -132.8511 | -132.6138 | -0.2373 |
| | -132.8497 | -132.6086 | -0.2411 |
| 4.125 | -132.8408 | -132.6031 | -0.2377 |
| | -132.8394 | -132.5964 | -0.243 |
| 4.13 | -132.8305 | -132.5923 | -0.2382 |
| | -132.8297 | -132.5860 | -0.2437 |
| 4.135 | -132.8211 | -132.5817 | -0.2394 |
| | -132.8194 | -132.5749 | -0.2455 |
| 4.140 | -132.8077 | -132.5690 | -0.2387 |
| | -132.8094 | -132.5657 | -0.2437 |

Table 2. Computations of E_{fm} , E_{exch}^{fm} , E_{afm} and E_{exch}^{afm} are done for lattice constant a in cubic BaTiO_3 . The units of energy are Hartree.

| $a(\text{\AA})$ | E_{exch}^{fm} | E_{exch}^{afm} | δ |
|-----------------|-----------------|------------------|----------|
| 4.00 | -138.4905 | -138.7541 | 0.2636 |
| | -138.7533 | -138.7532 | -0.0001 |
| 4.005 | -138.4785 | -138.7403 | 0.2618 |
| | -138.7396 | -138.7394 | -0.0002 |
| 4.01 | -138.4663 | -138.7265 | 0.2602 |
| | -138.7259 | -138.7125 | -0.0134 |
| 4.015 | -138.4546 | -138.7132 | 0.2586 |
| | -138.4554 | -138.7125 | 0.2571 |
| 4.02 | -138.4427 | -138.6996 | 0.2569 |
| | -138.6990 | -138.6989 | 0.0001 |

Table 3. Computations of E_{fm} , E_{exch} , E_{afm} and E_{exch} are done for lattice constant a in cubic BaVO_3 . The units of energy are Hartree.

| $a(\text{\AA})$ | E_{exch}^{fm} | E_{exch}^{afm} | δ |
|-----------------|-----------------|------------------|----------|
| 4.049 | -145.2346 | -143.9615 | -1.2731 |
| | -145.0421 | -143.9616 | -1.0805 |
| 4.054 | -145.2010 | -143.9488 | -1.2522 |
| | -145.2075 | -143.9489 | -1.2586 |
| 4.059 | -145.2231 | -143.9360 | -1.2871 |
| | -145.3132 | -143.9362 | -1.377 |
| 4.064 | -145.1868 | -143.9234 | -1.2634 |
| | -145.1926 | -143.9235 | -1.2691 |
| 4.069 | -145.1994 | -143.9108 | -1.2866 |
| | -145.1770 | -143.9110 | -1.266 |

Table 4. Computations of E_{fm} , E_{exch}^{fm} , E_{afm} , and E_{exch}^{afm} are done for lattice constant a in cubic BaCrO_3 . The units of energy are Hartree.

| $a(\text{\AA})$ | E_{exch}^{fm} | E_{exch}^{afm} | δ |
|-----------------|-----------------|------------------|----------|
| 3.8436 | -151.8259 | -150.3628 | -1.4631 |
| | -151.8267 | -150.3763 | |
| 3.8486 | -151.8586 | -150.3475 | -1.5111 |
| | -151.8283 | -150.3609 | |
| 3.8536 | -151.9614 | -150.3326 | -1.6288 |
| | -151.8653 | -150.3381 | |
| 3.8586 | -151.8034 | -150.3179 | -1.4855 |
| | -151.7902 | -150.3232 | |
| 3.8636 | -151.7371 | -150.3032 | -1.4339 |
| | -151.8065 | -150.3085 | |

Table 5. Computations of E_{fm} , E_{exch}^{fm} , E_{afm} and E_{exch}^{afm} are done for lattice constant a in cubic $BaMnO_3$. The units of energy are Hartree.

| $a(\text{\AA})$ | E_{exch}^{fm} | E_{exch}^{afm} | δ |
|-----------------|-----------------|------------------|----------|
| 3.80 | -34.8595 | -157.2687 | 122.4092 |
| | -156.8650 | -157.2736 | |
| 3.85 | -65.2846 | -156.8965 | 91.6119 |
| | -158.2801 | -156.9355 | |
| 3.90 | -159.0151 | -156.8844 | -2.1307 |
| | -157.9015 | -157.2532 | |
| 3.95 | -64.0915 | -157.2102 | 93.1187 |
| | -157.5813 | -156.9111 | |
| 4.00 | -159.0042 | -157.2003 | -1.8039 |
| | -157.6340 | -156.8992 | |

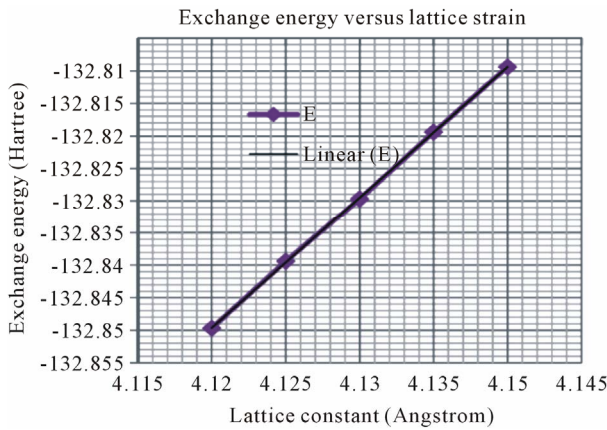


Figure 3. Exchange energy vs. lattice strain for cubic $BaScO_3$. A decrease in exchange energy can be seen for the compression of lattice. The straight line is drawn to signify the linearity of the trend.

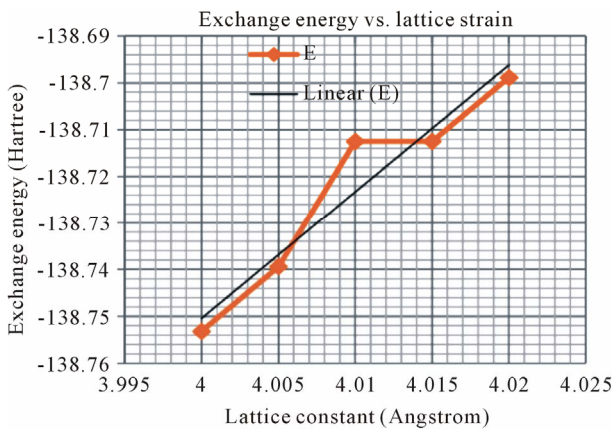


Figure 4. Exchange energy vs. lattice strain for cubic $BaTiO_3$. A decrease in exchange energy can be seen for the compression of lattice. There is smaller deviation from the linear trend.

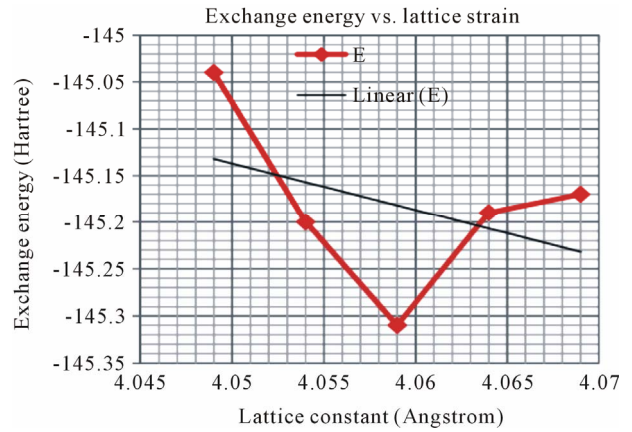


Figure 5. Exchange energy vs. lattice strain for cubic $BaVO_3$. A slight increase in the exchange energy can be seen for the compression of lattice. The nonlinear dependence of the exchange energy on lattice strain is more pronounced.

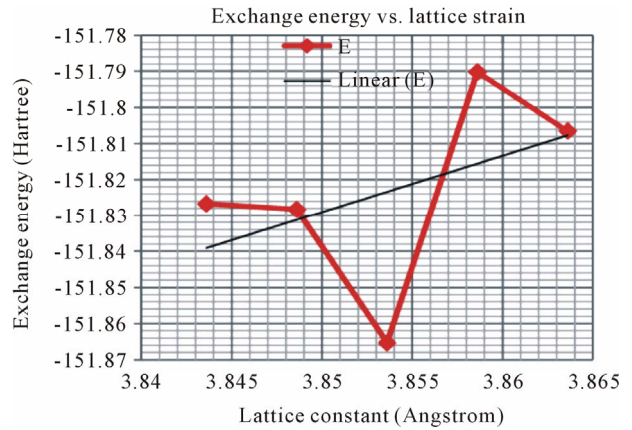


Figure 6. Exchange energy vs. lattice strain for cubic $BaCrO_3$. A decrease in exchange energy can be seen for the compression of lattice. The oscillatory character of exchange energy is also persistent.

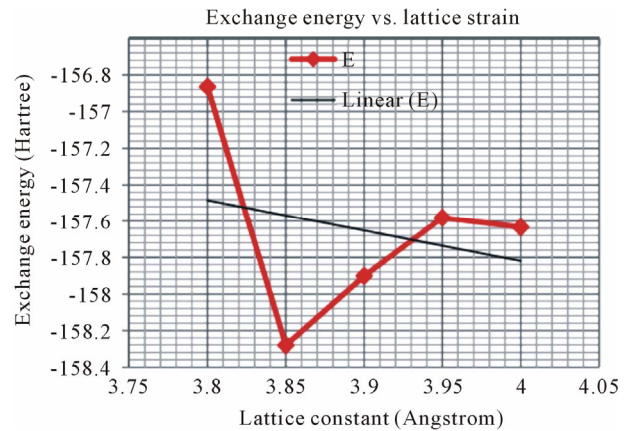


Figure 7. Exchange energy vs. lattice strain for cubic $BaMnO_3$. The nonlinear dependence of the exchange energy on the compression of lattice can be observed. Exchange energy has slightly increased with the compression of the lattice in this case.

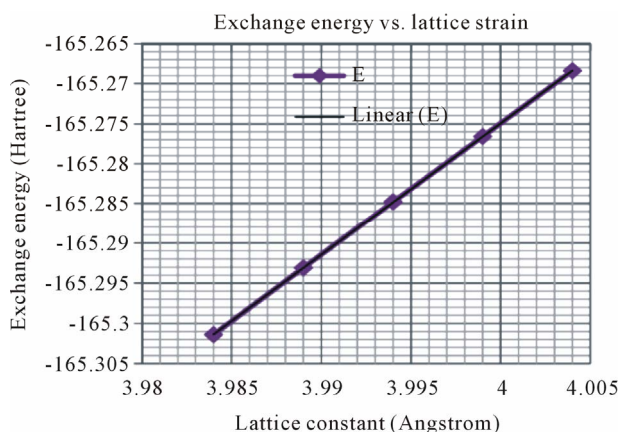


Figure 8. Exchange energy vs. lattice strain for cubic BaFeO₃. A decrease in exchange energy can be seen for the compression of lattice showing a linear dependence on the strain.

known as manganites perovskites. The crystalline geometry and properties of cubic BaMnO₃ may be well suited to the quantum mechanical model. These models advocate a delicate balance between the crystalline field and Hund's pairing energy. The crystalline field in these models originates due to a coulombic force between the electrons and atomic centers. The electrostatic fields partially attributed to these crystalline fields are intricately interdependent. The interaction between the crystalline field and Hund's pairing energy for the relaxed as well as the strained crystalline structures is interpreted from this model here. The phenomenon of ferromagnetic spin exchange, depending upon the highly correlated electrons in a crystal field, is also accommodated in the model. It is assumed that the ferromagnetic or antiferromagnetic properties due to electron spin polarization depend upon the crystal field of the strained lattice structure. This model can also be applied to manganites (AMnO₃), titanates (ATiO₃) and vanadates (AVO₃) as the crystal field splitting is predominant and is relevant in all the material systems discussed as in ref. [7].

The Hamiltonian for a typical transition metal oxide may be

$$H_{eff} = H_{hund} + H_{t_{2g}} + H_{e_g} \quad (1)$$

The H_{e_g} term in Equation (1) may express the energy component due to e_g valence electrons of the transition metals σ -bonded with the p -valence electrons for O atoms in placed in an octahedral complex. The $H_{t_{2g}}$ term expresses the energy component due to t_{2g} electron which are π -bonded the p -electrons of O atoms.

The term H_{hund} expresses the Hund energy for electrons

$$H_{hund} = J_H \sum_i S_i S_i^{t_{2g}} \quad (2)$$

The second energy component in Equation (1) is at-

tributed to electrons localized at t_{2g} suborbital

$$H_{t_{2g}} = J_{ij} S_i^{t_{2g}} S_j^{t_{2g}} \quad (3)$$

Equation (4) splits the H_{e_g} term further

$$H_{e_g} = \Delta \sum_i L_{iz} + \sum_{(ij)\sigma\gamma\gamma'} t_{ij}^{\gamma\gamma'} \gamma' (a_{i\gamma\sigma}^\dagger a_{j\gamma'\sigma}) + \sum_\beta H_{U_\beta} \quad (4)$$

In Equation (4), the subscripts i and j express the nearest neighbors on ionic sites, $a_{i\gamma\sigma}^\dagger$ and $a_{j\gamma'\sigma}$ are the creation and annihilation operators respectively. The term t in Equation (4) expresses the kinetic energy of e_g electrons in BaMnO₃, BaCrO₃ and BaFeO₃ and electrostatic energy term U . The Equation (4) takes into account the kinetic energy of electrons delocalized due to strains on the σ -bonded e_g and p -orbitals. The electrons hop between the cation and anion sites termed as i and j .

$$t = \sum_{(ij)\sigma\gamma\gamma'} t_{ij}^{\gamma\gamma'} \gamma' (a_{i\gamma\sigma}^\dagger a_{j\gamma'\sigma}) \quad (5)$$

$$t_{ij}^{\gamma\gamma'} = \alpha_{\gamma\gamma'} t_{oij} \quad (6)$$

The electrostatic energy term U expresses the on-site electron correlation in transition metal cations resulting in the electron localization on transition metal sites. The symbol t in Equation (5) is the hopping integral for electrons transferred under the action of strains between ions i and the nearest neighbors j . Hund's energy consists of energy components due to t_{2g} and e_g electrons which are well-localized on each transition metal site due to electron correlations as shown in Equation (7).

$$J_H = H_U + H_{U_{t_{2g}}} + H_{U_{e_g}} \quad (7)$$

It is assumed that the term $\Delta\varepsilon$ in Equation (8) may be related with the change in the crystal field energy originating due to external strain. The term $\sum_i T_i$ expresses the change in the orbital spin angular momentum due to the effect of strain.

$$\Delta\varepsilon = \Delta \sum_i T_i \quad (8)$$

3. Results and Discussion

The computational results are shown in **Tables 1-5** and **Figures 3-5**. It is observed that the computational values of energy due to spin polarizations are coupled with electronic structures. The results are also plotted in **Figures 3-5**. The oscillations in energy for the BaVO₃, BaCrO₃ and BaMnO₃ show that the coupling between the electronic structures and valence electrons are fairly complex. In **Tables 1-5**, the E_{fm} , E_{exch}^{fm} , E_{afm} and E_{exch}^{afm} represent the energies arising from ferromagnetic and antiferromagnetic spin polarizations.

The primary effect of the external pressure on the transition metal oxides is to compress or expand their

bond lengths connecting the transition metal and oxygen atoms in a perovskite. The expansion and contraction of the bond length result in the weakening or strengthening of the electron interactions within crystal structures among the transition metal e_g electrons and oxygen p electrons. The interactions between electrons and ions couple them in a complicated manner.

Moreover, these interactions are facilitated by the strains only if there are enough numbers of electrons in e_g valence orbitals. This phenomenon can be observed in the computational results obtained for BaCrO₃, BaMnO₃ and BaFeO₃. Less variations in energy as a function of lattice strains for some oxides is a function of the localized nature of the t_{2g} and e_g electron orbitals.

The oxides of transition metal have varied number of electrons in their highly correlated d -orbitals. The contracted wavefunctions of d electrons in BaScO₃, BaTiO₃, BaVO₃, BaMnO₃ and BaFeO₃ experience the varied degree of competitive forces of the coulomb repulsion versus hybridization. The former tries to localize the electrons at atomic lattice sites while the latter favors the overlaps with p - and d -orbitals of O and transition metal to delocalize these electrons. The forces of coulomb repulsion and hybridization are varied by lattice strain. A trend can be seen in all computations as there is a consistent decrease in energy for the compression and increase in energy for expansion of lattice volume. The chemical bond in transition metal oxides is a combination of covalent and ionic parts. The covalent and ionic parts vary as the transition metal ionic radius increases from Sc to Fe. The contribution of ionic bonding is increased as the number of electrons in transition metals are increased with more impact on the energy as a function of lattice strain. The computational results of BaScO₃, BaTiO₃, BaVO₃, BaCrO₃, BaFeO₃ show significant variations in chemical bonding from strongly covalent to moderately ionic in nature for the materials tested.

From the computed results shown in **Tables 1-6**, an increase in the energy is observed for spins polarized in same direction for all crystalline systems tested confirming the coupling between the crystalline structure and electron spin polarization.

4. Concluding Remarks

We have employed first principles computations to extract the coupling between the crystalline structure and electron spin polarization. The optimized crystalline structures are computed by a variety of methods for each of the transition metal oxides. Later on, the coupling between the electronic structure and electron spin polarization is determined by computing the energy for the spins aligned in the parallel as well as antiparallel polariza-

Table 6. Computations of E_{fm} , E_{exch}^{fm} , E_{afm} , and E_{exch}^{afm} are done for lattice constant a in cubic BaFeO₃. The units of energy are Hartree.

| a (Å) | E_{exch}^{fm} | E_{exch}^{afm} | δ |
|---------|-----------------|------------------|----------|
| 3.984 | -165.3002 | -164.6210 | -0.6792 |
| | -165.3014 | -164.6329 | -0.6685 |
| 3.989 | -165.2919 | -164.6123 | -0.6796 |
| | -165.2931 | -164.6254 | -0.6677 |
| 3.994 | -165.2836 | -164.6046 | -0.679 |
| | -165.2848 | -164.6173 | -0.6675 |
| 3.999 | -165.2754 | -164.5965 | -0.6789 |
| | -165.2766 | -164.6092 | -0.6674 |
| 4.004 | -165.2673 | -164.5896 | -0.6777 |
| | -165.2684 | -164.6020 | -0.6664 |

tions. It is observed that the compression of the the bulk crystal results in the lowering of the the energy confirming the fact that the former is intricately coupled with the latter.

It is seen that the coupling between the electronic structure and electronic polarization varies with the occupation of electrons in the outermost orbitals. During computations, it has been observed that the compression lowers the electron energy in the transition metal oxides of Sc-Fe. The lowering of the polarization energy may be attributed to the stronger coupling between transition metal e_g and O p -orbitals forming a σ -bond.

5. Acknowledgements

One of the authors (WFP) gratefully acknowledges the support of the Office of Naval Research Grant N00014-01-1-0802 through the MURI program.

REFERENCES

- [1] R. Gopalan and V. Chandrasekharan, "Room temperature multiferroism and magnetoelectric coupling in BaTiO₃-BaFe₁₂O₁₉ System Srinivas," *Solid State Communications*, Vol. 149, No. 9-10, 2009, pp. 367-370.
- [2] J. P. Velev, P. A. Dowben, E. Y. Tsymlal, S. J. Jenkin, and A. Caruso, "Interface Effects in Spin-Polarized Metal/Insulator Layered Structures," *Surface Science Reports*, Vol. 63, No. 9, 2008, pp. 400-425.
[doi:10.1016/j.surfrep.2008.06.002](https://doi.org/10.1016/j.surfrep.2008.06.002)
- [3] J. B. Goodenough, "Electron-Lattice Interactions in Manganese-Oxide," *Perovskites, Fundamental Materials Research*, 2002, pp. 127-133.
- [4] C. N. R. Rao, "Transition Metal Oxides," *Annual Review of Physical Chemistry*, Vol. 40, 1989, pp. 291-326.

[doi:10.1146/annurev.pc.40.100189.001451](https://doi.org/10.1146/annurev.pc.40.100189.001451)

- [5] S. Horiuchi, Y. Okimoto, R. Kumai and Y. Tokura, "Quantum Phase Transition in Organic Charge-Transfer Complexes," *Science*, Vol. 299, 2003.
- [6] J. P. Velev, C.-G. Duan, J. D. Burton, A. Smogunov, M. K. Niranjan, E. Tosatti, S. S. Jaswal and E. Y. Tsybal, "Magnetic Tunnel Junctions with Ferroelectric Barriers: Prediction of Four Resistance States from First Principles," *Nano Letters*, Vol. 9, No. 1, 2009, pp. 427-432. [doi:10.1021/nl803318d](https://doi.org/10.1021/nl803318d)
- [7] I. Sumio, O. Satoshi and M. Sadamichi, *Physics of Transition Metal Oxides*, 1997.
- [8] Y. Tokura and N. Nagaosa, "Orbital Physics in Transition-Metal Oxides," *Science*, Vol. 288, No. 462, 2000, pp. 462-468.